JACS
JOURNAL OF THE AMERICAN CHEMICAL SOCIETY

Communication

pubs.acs.org/JACS

Two-Dimensional Metal–Organic Surfaces for Efficient Hydrogen Evolution from Water

Andrew J. Clough,[†] Joseph W. Yoo,[†] Matthew H. Mecklenburg,[‡] and Smaranda C. Marinescu*[,†]

[†]Department of Chemistry and [‡]Center for Electron Microscopy and Microanalysis, University of Southern California, Los Angeles, California 90089, United States

Supporting Information

ABSTRACT: Hydrogen production through the reduction of water has emerged as an important strategy for the storage of renewable energy in chemical bonds. One attractive scenario for the construction of efficient devices for electrochemical splitting of water requires the attachment of stable and active hydrogen evolving catalysts to electrode surfaces, which remains a significant challenge. We demonstrate here the successful integration of cobalt dithiolene catalysts into a metal–organic surface to generate very active electrocatalytic cathode materials for hydrogen generation from water. These surfaces display high catalyst loadings and remarkable stability even under very acidic aqueous solutions.

Energy harvested directly from sunlight offers a desirable approach toward fulfilling the global need for clean energy.[1] Hydrogen produced through the reduction of water is an attractive candidate as a clean and renewable fuel. Much work has gone into developing homogeneous and heterogeneous hydrogen evolving catalysts made from nonprecious metals for applications in efficient, scalable energy storage. A variety of base metals homogeneous[2] and heterogeneous[3] hydrogen evolving catalysts have been developed recently. The construction of efficient and practical devices for electrocatalytic splitting of water requires the attachment to electrodes of hydrogen evolving catalysts based on nonprecious metals that can operate and are robust under acidic aqueous conditions, under which proton exchange membrane-based electrolysis is operational.[4] A variety of cobalt species have been adsorbed onto the electrodes by controlled potential electrolysis and display H_2-evolving activity.[5] Molecular catalysts are attractive because the ligand environment allows for tuning of their reduction potentials and chemical properties. However, the reported methods for the immobilization of molecular catalysts onto electrodes are scarce. Demonstrated grafting methods include the covalent attachment of nickel[4a,6] or cobalt complexes[7] onto carbon-based supports (multiwalled carbon nanotubes or glassy carbon), the coordination of cobaloximes to vinylpyridine GaP surfaces,[8] and the immobilization of molecular catalysts via pyrene groups.[9] However, these methods suffer from low coverage; the maximum catalyst loading achieved is 10^{-8} $mol_{catalyst}/cm^2$.[9b] The attachment of catalysts to surfaces in a well-defined fashion remains a great challenge. Incorporation of active sites in an extended catalytic surface was envisioned to maintain the properties of the molecular catalysts such as activity and reduction potential, while also increasing the catalyst loading and rendering the material more robust and transferable to an electrode surface by direct deposition.

Two-dimentional (2D) covalent– or metal–organic frameworks (COFs/MOFs) afford control of atomic layers deposited on surfaces.[10] These materials can be grown on a variety of supports and are characterized by high charge carrier mobility and high surface-to-volume ratio. Moreover, the heterogeneous nature of the COFs/MOFs allows for easy separation, reusability, and enhanced stability, making them attractive in the context of developing integrated photoanode and photocathode materials in a solar fuel cell. However, despite their great promise, the catalytic properties of these nanoscopic architectures have not been described. We report here the development of metal–organic surfaces (MOS) and their applications as efficient electrode materials for the reduction of acidic water.

Cobalt dithiolene species are among the most efficient molecular catalysts for the hydrogen evolution reaction (HER).[11] Related nickel dithiolenes species have been investigated as well for HER;[12] however, their chemistry is under debate.[11a,13] In order to access extended architectures with integrated cobalt dithiolene catalytic sites, a trinucleating conjugated ligand, benzenehexathiol (BHT), was employed in reactions with cobalt(II) through a liquid–liquid interfacial process (Scheme 1). An acetonitrile/ethyl acetate solution of $[Co(MeCN)_6][BF_4]_2$ was gently layered on top of an aqueous solution of sodium benzenehexathiolate ($C_6S_6Na_6$). The organic solvents were allowed to evaporate over 1 h, leaving behind a black film (**1**) at the gas–liquid interface. Film **1** can be deposited on a variety of supports, such as glassy carbon or highly oriented pyrolytic graphite (HOPG), by immersing the support face down into the reaction mixture. The generated MOS **1** was washed and dried. Additionally, the black powder was collected on a fine porosity frit and washed with water and methanol. The measured elemental composition of the black powder corresponds to a molecular formula of $(CoC_4S_4Na)_n$. This method has been extended to frameworks based on triphenylene-2,3,6,7,10,11-hexathiolate (**2**). Powder X-ray diffraction (PXRD) studies of **2**, obtained by method A (see Supporting Information (SI)), revealed a crystalline structure with peaks at $2\theta = 4.5$, 9.1, 12.0 and 15.6°, indicative of long-range order within the *ab* planes (Figure S28, SI). The peak at $2\theta = 4.5°$ corresponds to a distance of ~20 Å, which is equal to the value expected for the pore diameter of MOF **2** determined using known bond lengths and

Received: November 13, 2014
Published: December 19, 2014

DOI: 10.1021/ja5116937
J. Am. Chem. Soc. 2015, 137, 118–121

Scheme 1. Synthesis of the Cobalt Dithiolene Films, 1 and 2, through a Liquid–Liquid Interfacial Reaction; the Synthesized Films Are Deposited onto the Desired Supports, Generating the MOS 1 and 2

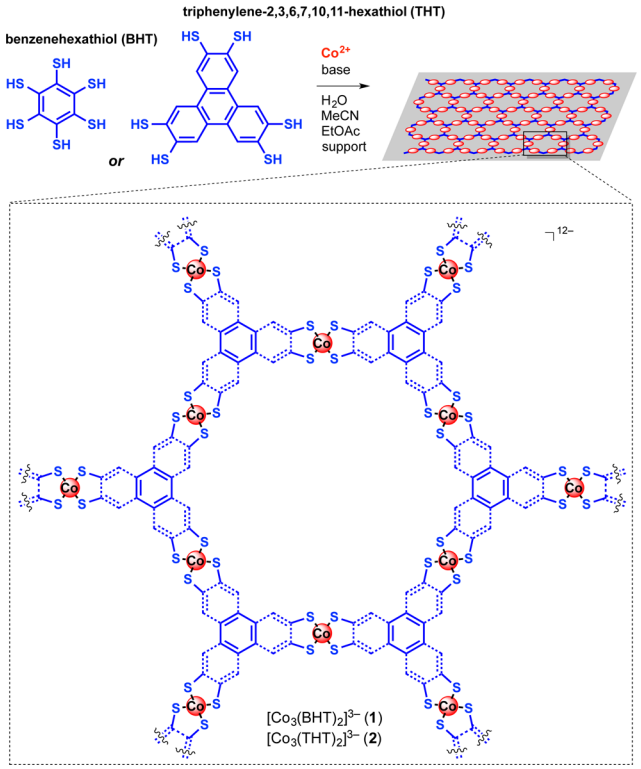

angles for molecular cobalt dithiolene species. An additional weaker and broader peak at $2\theta = 26.7°$ is indicative of poorer long-range order along the *c* direction, as expected for layered materials. A similar PXRD pattern has been reported for layered MOF Ni_3(2,3,6,7,10,11-hexaiminotriphenylene)$_2$.[10g] UV–vis spectra of **1** and **2** display broad bands between 270 and 600 nm wavelengths, analogous with the UV–vis spectra of MOF Ni_3(2,3,6,7,10,11-hexaiminotriphenylene)$_2$.[10g] The FTIR spectra of **1** and **2** show the disappearance of the strong signal present in the hexathiols at 2500 cm^{-1}, which corresponds to the S–H stretching vibration (Figure S2, SI).

X-ray photoelectron spectroscopy (XPS) analysis of MOS **1** revealed the presence of Co, S, and Na (Figure S3, SI). Two sets of peaks are observed in the cobalt region, with binding energies of ~780 and ~795 eV, which correspond to the $2p_{3/2}$ and $2p_{1/2}$ levels in the expected 2:1 ratio. Deconvolution of these signals generates four peaks; the peaks at 779.2 and 794.2 eV are assigned to Co^{III}, whereas the ones at 780.9 and 795.4 eV are assigned to Co^{II}.[14] This assignment is in agreement with the electronic structure of cobalt bisdithiolene complexes, which was interrogated by a variety of spectroscopic and theoretical studies, and is best represented by the resonances $[Co^{III}(bdt)_2]^{-1} \leftrightarrow [Co^{II}(bdt)(bdt^{\bullet})]^{-1}$ (bdt =1,2-benzenedithiolate).[15] Three additional peaks are observed with binding energies of 1071.4, ~228, and ~163 eV, which correspond to Na 1s, S 2s, and S 2p, respectively. The broad peaks at 230.0 and 166.0 eV are assigned to the shape-up satellites, which are often observed in bisdithiolene complexes.[10d,16] XPS analysis of MOS **2** revealed similar peaks with the ones observed for **1** (Figures S4 and S5, SI). These data support assignment of the MOS with cobalt dithiolene moieties linked by hexathiolate nodes.

The coverage and thickness of the film on HOPG was evaluated by scanning electron-microscopy (SEM). A top-down micrograph is illustrated in Figure S29a, SI. Cross-sectional micrographs were obtained after depositing a protective layer of Pt and milling the sample with a Ga^+ focused ion beam (FIB). The cross section of the film revealed an average thickness of 360(40) nm. The average surface catalyst concentration of MOS **1**, determined using the electrochemical methods described below, was $3.7(4) \times 10^{-6}$ mol_{Co}/cm^2. Detection of the electron diffraction from MOS **1**, using select area electron diffraction (SAED) techniques, was inhibited by the film's beam sensitivity (the images lasted less than 200 ms). The electron diffraction pattern of MOS **1** on silicon nitride membranes displays a hexagonal symmetry, suggesting that the material is weakly crystalline (Figure S29b, SI). Similar patterns were detected at several locations in the sample. Elemental mapping of cobalt and sulfur using SEM–energy dispersive spectroscopy (SEM–EDS) are illustrated in Figure S29c–e, SI, indicating that these elements are homogeneously distributed and colocalized throughout the film.

The electrochemistry of MOS **1** was investigated by cyclic voltammetry (Figure 1). When the MOS-modified glassy carbon electrode was immersed in pH 10.0 buffer, a broad reversible redox couple was observed, with an E° of −0.30 V vs SHE (−0.50 V vs SCE). The peak current was directly proportional to the scan rate over the range of 1–100 mV/s (Figures S8–9, SI). The

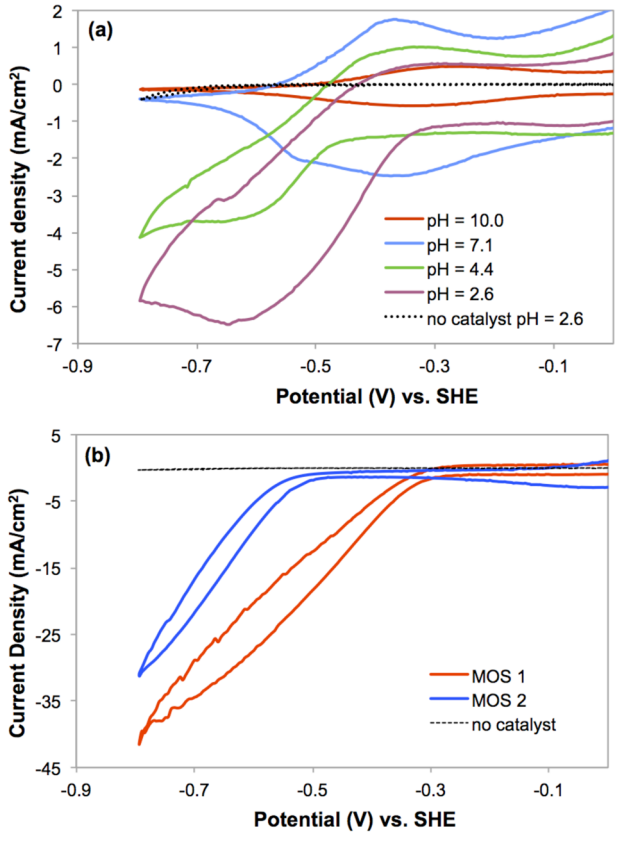

Figure 1. Electrochemical studies of MOS **1** and **2**. (a) Polarization curves of MOS **1** ($1.9(2) \times 10^{-6}$ mol_{Co}/cm^2) in 0.1 M $NaClO_4$ aqueous solutions at pH 10.0 (red), 7.1 (blue), 4.4 (green), 2.6 (purple), and of blank glassy carbon electrode at pH 2.6 (dashed black); scan rate, 20 mV/s. (b) Polarization curves of MOS **1** (red, $0.7(1) \times 10^{-6}$ mol_{Co}/cm^2) and MOS **2** (blue, method B, $1.1(1) \times 10^{-6}$ mol_{Co}/cm^2) in pH 1.3 H_2SO_4 solution; scan rate, 100 mV/s.

DOI: 10.1021/ja5116937
J. Am. Chem. Soc. 2015, 137, 118–121

peak separation (ΔE_p) is small (<20 mV) at scan rates below 10 mV/s, indicative of rapid electron transfer between the glassy carbon electrode and MOS **1**. At higher scan rates (10−100 mV/s), the separation between the reduction and oxidation peaks increases with the scan rate. The observed voltammetric profile is indicative of a surface-confined redox couple. The value of the redox couple for MOS **1** is similar to the one reported for the molecular analogue, $Co(bdt)_2^-$, which was observed at −0.64 V vs SCE in 1:1 H_2O/MeCN solutions, and assigned to $Co(bdt)_2^{-1/-2}$.[11a,b,17] Maximum average surface catalyst concentrations are similar for MOS **1** and **2** ($3.7(4) \times 10^{-6}$ mol_{Co}/cm^2 for MOS **1**, and $2.5(3) \times 10^{-6}$ mol_{Co}/cm^2 for MOS **2**), as estimated from the integration of the electrochemical wave at pH 10.0. Similar values are obtained from ICP−MS measurements of the digested catalyst films, suggesting that the majority of the cobalt centers are electrochemically active.

As the pH of the aqueous solution is lowered, an increase in current is observed (Figure 1a), indicating that a catalytic reaction is taking place. A peak-shaped catalytic current was observed at −0.65 V vs SHE at pH 2.6 for MOS **1**. A potential value of −0.51 V vs SHE (−0.35 V vs RHE) was required to reach a current density of 5 mA/cm^2 at pH 2.6. By comparison, unmodified glassy carbon electrodes display insignificant increase in current. The solutions that resulted after the electrochemical studies of MOS **1** at each pH were subjected to cyclic voltammetry in the presence of a blank glassy carbon electrode. Negligible current densities were observed, indicating that the modified electrode does not generate soluble materials responsible for catalysis. Additionally, ICP−MS measurements indicate that the amount of cobalt present in solution is negligible.

At the lowest pH value (pH = 1.3), and in the presence of MOS **1** or MOS **2**, large current densities can be observed (41 and 31 mA/cm^2 for MOS **1** and **2**, respectively, at −0.8 V vs SHE) (Figure 1b). It is noteworthy that the voltammograms of the MOS **1** and **2** at pH 1.3 are distinct. The measured onset for H_2-evolution for MOS **1** is at −0.28 V vs SHE, whereas for MOS **2** is at −0.48 V vs SHE, suggesting that the active material is not identical for MOS **1** and **2**. Catalytic current densities of MOS **1** and **2**, measured at potentials of −0.55 and −0.85 V vs SHE, respectively, increase linearly with catalyst loading (Figures S13 and S14, SI). Tafel analyses of MOS **1** and **2** gave Tafel slopes between 149 and 189 mV/dec, and exchange current densities of $10^{-5.3(1)}$ A/cm^2 at pH 4.2 (Figures S15 and S16, SI), which are comparable to the ones reported for cobalt complexes grafted onto amine-modified multiwalled carbon nanotubes.[7] Glassy carbon electrodes modified with starting materials only (cobalt(II) or thiolates) display insignificant increase in current. The activities of MOS **1** and **2** were compared to that of the molecular analogue, $[Co(bdt)_2]$ (Figure S18 and Table S1, SI). Glassy carbon electrodes modified with $[Co(bdt)_2]^-$ by the drop-casting method or in solution display a very small increase in current, suggesting that immobilization via MOS provides an increase in activity and stability.

Controlled potential electrolysis of MOS **1** on a glassy carbon electrode in 0.1 M $NaClO_4$ citrate/phosphate buffer at pH 2.6 and −0.8 V vs SHE consumed 45 coulombs of charge after 2 h (Figure S19, SI). Analysis of the gas mixture in the headspace of the working compartment of the electrolysis cell by gas chromatography confirmed production of H_2 with a Faradaic yield of 97 ± 3%. In the presence of MOS **1** and a mixture of $NaClO_4$/$HClO_4$ at pH 1.0 and −0.8 V vs SHE, 57 coulombs of charge were consumed in 1 h. The durability of MOS **1** in pH 2.6 aqueous solution was further assessed in a longer-duration controlled potential electrolysis experiment. MOS **1** affords a continuous increase in charge build-up over a 10 h controlled potential electrolysis at −0.55 or −0.65 V vs SHE (Figures S20 and S21, SI). As H_2 bubbles generated during the 10 h controlled potential electrolysis cause the peeling-off of the material, the decrease in catalyst loading leads to some lowering in current flow. XPS analyses of MOS **1** and **2** after electrochemical studies display peaks similar to the ones observed before electrolysis, suggesting that the material is stable under reductive and acidic conditions (Figures S22−24, SI). By comparison, unmodified glassy carbon electrodes display insignificant H_2-evolution activity.

To test whether the molecular cobalt dithiolene species decomposes during catalysis to generate a heterogeneous material active for H_2-evolution, the following control experiment was performed. Cyclic voltammograms of a 0.3 mM solution of $[Co(bdt)_2]^-$ in a 1:1 mixture of pH 1.3 aqueous H_2SO_4 solution and 0.1 M KNO_3 acetonitrile solution display a maximum current density of 6.0 mA/cm^2 at −0.63 V vs SHE (Figure S25, SI). The electrode was then rinsed with water and MeCN several times to remove any physisorbed complex and transferred to a fresh 1:1 mixture. The observed current densities of the rinsed electrode were negligible, suggesting that $[Co(bdt)_2]^-$ does not decompose during catalysis to generate a heterogeneous material active for H_2-evolution.

The materials prepared here operate under fully aqueous conditions. Overpotentials of 0.34 and 0.53 V are required for MOS **1** and **2**, respectively, to reach current densities of 10 mA/cm^2 at pH 1.3. In comparison, other immobilized H_2-evolving catalysts require much higher overpotentials to reach current densities of 10 mA/cm^2.[7] Similar overpotentials to the ones observed here have been reported for molecular cobalt dithiolene complexes in mixtures of aqueous and organic solvents suggesting that, although in an extended material, the environment around cobalt maintains the properties of the molecular catalyst.[11a,b] This feature is important for further rational tuning of reactivity. The maximum average surface catalyst concentration observed for MOS **1** is $3.7(4) \times 10^{-6}$ mol_{Co}/cm^2, which is 2 orders of magnitude higher than the maximum catalyst loading reported.[9b] This high surface concentration is indicative of a multilayered material. In addition to the low overpotential, the high catalyst loading and activity, MOS **1** displays remarkable stability under acidic conditions, and moderate durability in longer-duration controlled potential electrolysis. Theoretical studies performed on the molecular cobalt dithiolene species suggest that the mechanism of hydrogen evolution involves protonation of the sulfur sites on the dithiolene ligands after the initial $Co^{III/II}$ reduction.[11c,17] This may eventually lead to ligand loss and decomposition in molecular systems. The high stability observed here for MOS **1** is ascribed to the network environment. Enhanced photochemical hydrogen production was also reported for a molecular diiron benzenedithiolate catalyst incorporated into a metal−organic framework.[18]

Cobalt dithiolene species are among the most efficient molecular catalysts for hydrogen evolution.[11] We demonstrate here the successful integration of the cobalt dithiolene catalysts into MOS to give very active electrocatalytic cathode materials for hydrogen generation from fully aqueous solutions. The materials generated display high catalyst loadings and remarkable stability under acidic conditions. These results indicate that immobilization as MOS provides a significant increase in activity

DOI: 10.1021/ja5116937
J. Am. Chem. Soc. 2015, 137, 118−121

and stability for these cobalt catalysts and thus paves the way toward development of practical devices.

■ ASSOCIATED CONTENT

Supporting Information

Experimental procedures, spectroscopic characterization, and electrochemical data. This material is available free of charge via the Internet at http://pubs.acs.org.

■ AUTHOR INFORMATION

Corresponding Author

*smarines@usc.edu

Notes

The authors declare no competing financial interest.

■ ACKNOWLEDGMENTS

We are grateful to the University of Southern California (USC) and the Office of the Provost of USC (Zumberge Individual award to S.C.M.) for funding. We thank Harry B. Gray, Mark E. Thompson, and Chi H. Mak for facilitating the initial stages of the project by providing access to laboratory space and equipment. We thank Beatriz J. Garcia-Barboza for the synthesis of a batch of ligand precursor, Noah Bodzin for assistance with the preparation of the FIB samples, and Courtney Downes for assistance with the ICP measurements. XPS, SEM, and TEM data were collected at the Molecular Materials Research Center of the Beckman Institute of the California Institute of Technology and the Center for Electron Microscopy and Microanalysis, USC.

■ REFERENCES

(1) (a) Lewis, N. S.; Nocera, D. G. *Proc. Natl. Acad. Sci. U.S.A.* **2006**, *103*, 15729. (b) Gray, H. B. *Nat. Chem.* **2009**, *1*, 7.

(2) (a) Dempsey, J. L.; Brunschwig, B. S.; Winkler, J. R.; Gray, H. B. *Acc. Chem. Res.* **2009**, *42*, 1995. (b) Artero, V.; Chavarot-Kerlidou, M.; Fontecave, M. *Angew. Chem., Int. Ed. Engl.* **2011**, *50*, 7238. (c) Du, P.; Eisenberg, R. *Energy Environ. Sci.* **2012**, *5*, 6012. (d) McKone, J. R.; Marinescu, S. C.; Brunschwig, B. S.; Winkler, J. R.; Gray, H. B. *Chem. Sci.* **2014**, *5*, 865. (e) Thoi, V. S.; Sun, Y.; Long, J. R.; Chang, C. J. *Chem. Soc. Rev.* **2013**, *42*, 2388. (f) Darensbourg, M. Y.; Lyon, E. J.; Zhao, X.; Georgakaki, I. P. *Proc. Natl. Acad. Sci. U.S.A.* **2003**, *100*, 3683. (g) Helm, M. L.; Stewart, M. P.; Bullock, R. M.; DuBois, M. R.; DuBois, D. L. *Science* **2011**, *333*, 863.

(3) Cook, T. R.; Dogutan, D. K.; Reece, S. Y.; Surendranath, Y.; Teets, T. S.; Nocera, D. G. *Chem. Rev.* **2010**, *110*, 6474.

(4) (a) Le Goff, A.; Artero, V.; Jousselme, B.; Tran, P. D.; Guillet, N.; Metaye, R.; Fihri, A.; Palacin, S.; Fontecave, M. *Science* **2009**, *326*, 1384. (b) Hambourger, M.; Gervaldo, M.; Svedruzic, D.; King, P. W.; Gust, D.; Ghirardi, M.; Moore, A. L.; Moore, T. A. *J. Am. Chem. Soc.* **2008**, *130*, 2015.

(5) (a) Berben, L. A.; Peters, J. C. *Chem. Commun.* **2010**, *46*, 398. (b) Sun, Y.; Liu, C.; Grauer, D. C.; Yano, J.; Long, J. R.; Yang, P.; Chang, C. J. *J. Am. Chem. Soc.* **2013**, *135*, 17699. (c) Cobo, S.; Heidkamp, J.; Jacques, P.-A.; Fize, J.; Fourmond, V.; Guetaz, L.; Jousselme, B.; Ivanova, V.; Dau, H.; Palacin, S.; Fontecave, M.; Artero, V. *Nat. Mater.* **2012**, *11*, 802. (d) Anxolabéhere-Mallart, E.; Costentin, C.; Fournier, M.; Nowak, S.; Robert, M.; Savéant, J.-M. *J. Am. Chem. Soc.* **2012**, *134*, 6104.

(6) Das, A. K.; Engelhard, M. H.; Bullock, R. M.; Roberts, J. A. S. *Inorg. Chem.* **2014**, *53*, 6875.

(7) Andreiadis, E. S.; Jacques, P.-A.; Tran, P. D.; Leyris, A.; Chavarot-Kerlidou, M.; Jousselme, B.; Matheron, M.; Pécaut, J.; Palacin, S.; Fontecave, M.; Artero, V. *Nat. Chem.* **2013**, *5*, 48.

(8) (a) Krawicz, A.; Yang, J.; Anzenberg, E.; Yano, J.; Sharp, I. D.; Moore, G. F. *J. Am. Chem. Soc.* **2013**, *135*, 11861. (b) Krawicz, A.; Cedeno, D.; Moore, G. F. *Phys. Chem. Chem. Phys.* **2014**, *16*, 15818.

(9) (a) Blakemore, J. D.; Gupta, A.; Warren, J. J.; Brunschwig, B. S.; Gray, H. B. *J. Am. Chem. Soc.* **2013**, *135*, 18288. (b) Tran, P. D.; Le Goff, A.; Heidkamp, J.; Jousselme, B.; Guillet, N.; Palacin, S.; Dau, H.; Fontecave, M.; Artero, V. *Angew. Chem.* **2011**, *50*, 1371.

(10) (a) Cote, A. P.; Benin, A. I.; Ockwig, N. W.; O'Keeffe, M.; Matzger, A. J.; Yaghi, O. M. *Science* **2005**, *310*, 1166. (b) Makiura, R.; Motoyama, S.; Umemura, Y.; Yamanaka, H.; Sakata, O.; Kitagawa, H. *Nat. Mater.* **2010**, *9*, 565. (c) Colson, J. W.; Woll, A. R.; Mukherjee, A.; Levendorf, M. P.; Spitler, E. L.; Shields, V. B.; Spencer, M. G.; Park, J.; Dichtel, W. R. *Science* **2011**, *332*, 228. (d) Kambe, T.; Sakamoto, R.; Hoshiko, K.; Takada, K.; Miyachi, M.; Ryu, J. H.; Sasaki, S.; Kim, J.; Nakazato, K.; Takata, M.; Nishihara, H. *J. Am. Chem. Soc.* **2013**, *135*, 2462. (e) So, M. C.; Jin, S.; Son, H.-J.; Wiederrecht, G. P.; Farha, O. K.; Hupp, J. T. *J. Am. Chem. Soc.* **2013**, *135*, 15698. (f) Cui, J.; Xu, Z. *Chem. Commun.* **2014**, *50*, 3986. (g) Sheberla, D.; Sun, L.; Blood-Forsythe, M. A.; Er, S.; Wade, C. R.; Brozek, C. K.; Aspuru-Guzik, A.; Dinca, M. *J. Am. Chem. Soc.* **2014**, *136*, 8859.

(11) (a) McNamara, W. R.; Han, Z.; Alperin, P. J.; Brennessel, W. W.; Holland, P. L.; Eisenberg, R. *J. Am. Chem. Soc.* **2011**, *133*, 15368. (b) McNamara, W. R.; Han, Z.; Yin, C.-J.; Brennessel, W. W.; Holland, P. L.; Eisenberg, R. *Proc. Natl. Acad. Sci. U.S.A.* **2012**, *109*, 15594. (c) Eckenhoff, W. T.; McNamara, W. R.; Du, P.; Eisenberg, R. *Biochim. Biophys. Acta* **2013**, *1827*, 958. (d) Han, Z.; Eisenberg, R. *Acc. Chem. Res.* **2014**, *47*, 2537. (e) Letko, C. S.; Panetier, J. A.; Head-Gordon, M.; Tilley, T. D. *J. Am. Chem. Soc.* **2014**, *136*, 9364.

(12) (a) Begum, A.; Moula, G.; Sarkar, S. *Chem.—Eur. J.* **2010**, *16*, 12324. (b) Fang, M.; Engelhard, M. H.; Zhu, Z.; Helm, M. L.; Roberts, J. A. S. *ACS Catal.* **2014**, *4*, 90.

(13) McCarthy, B. D.; Martin, D. J.; Rountree, E. S.; Ullman, A. C.; Dempsey, J. L. *Inorg. Chem.* **2014**, *53*, 8350.

(14) Chuang, T. J.; Brundle, C. R.; Rice, D. W. *Surf. Sci.* **1976**, *1976*, 413.

(15) Sproules, S.; Wieghardt, K. *Coord. Chem. Rev.* **2011**, *255*, 837.

(16) (a) S.-G, L.; Liu, Y.-Q.; Zhu, D.-B. *Synth. Met.* **1997**, *89*, 187. (b) Zhou, S.; Ichimura, K.; Inokuchi, H. *J. Mater. Chem.* **1995**, *5*, 1725.

(17) Solis, B. H.; Hammes-Schiffer, S. *J. Am. Chem. Soc.* **2012**, *134*, 15253.

(18) Pullen, S.; Fei, H.; Orthaber, A.; Cohen, S. M.; Ott, S. *J. Am. Chem. Soc.* **2013**, *135*, 16997.

DOI: 10.1021/ja5116937
J. Am. Chem. Soc. 2015, 137, 118−121